

Influence of Fluid Properties on Oil Drainage Multiphase Flow in a Complex Pore Network

Joseph Sinchitullo, MSc.¹, César Celis, PhD.², Guillermo Prudencio, MSc.¹ and Antony Sinchitullo, Ing.¹

¹Universidad Nacional de Ingeniería, Perú, jsinchitullo@uni.pe, gprudenciob@uni.pe, vsinchitullo@uni.pe

²Pontificia Universidad Católica del Perú, Perú, ccelis@pucp.edu.pe

Abstract— Fluid flow as two-phase in porous media is found in many processes, for example in enhanced oil recovery (EOR). That is why understanding the flow behavior at the pore scale is essential for the efficient exploitation of an oil reservoir. The fluid properties modeling is modeled for oil drainage systems, in which the investigation measures the main factor that affects the fluid behavior in a complex pore network, mainly focused on Reynolds number, and capillary pressure. In this study, the Darcy-Brinkman multiphase approach will be used, using an open-source in OpenFOAM to simulate two-phase flow for a complex pore network, including regions without solids and porous matrices. The main results indicate that fluid properties have an important impact on oil drainage, by reducing the volume of oil recovery due to the presence of the solid region. The fluid properties influenced the fluid flow in a complex porous medium, it is observed when the Reynold number was changed, and this behavior is in concordance of fluid flow at the microscale (pore-scale).

Keywords—Multiphase Flow, Oil Drainage, Enhanced Oil Recovery, Pore Network, OpenFOAM.

I. INTRODUCTION

Multiphase fluid dynamics in complex porous media plays a key role in natural flows in the reservoir to increase the recovery factor, such as enhanced oil recovery (EOR) and involves strong interaction between inertial, viscous, capillaries, and interfacial forces [1]. Mainly, the multiphase flow and its displacement are controlled by the behavior of the fluid at the pore scale [2]. The flow dynamics of multiphase fluids have been studied both experimentally and numerically [3], [4]. It is necessary to understand the complex link between microscopic geometric heterogeneities and macroscopic processes. Therefore, scale-dependent processes through the porous medium must be considered to generate predictive models: on the scale of micro-interfaces (μm) to the scale of complex pore networks [5]. Carrillo et. to the. [5] implemented an alternative solution to the scaling process, for which they suggest applying a single equation to control flow and transport in systems where the large-scale free solid domain coexists with a reduced volume porous domain (Fig. 1). Navier-Stokes equations should be averaged over a control volume containing both fluids and solids, using the multiphase Darcy-Brinkman (DB) approach to simulate two-phase flow for a complex pore network. On the other hand, Horgue et al. [6] proposed the first two-phase micro continuous model, for this they made a combination between the two-phase model of

DB equation with the volume of fluid (VOF) approach, this for the two-phase flow in the free regions of solids. Subsequently, Soulaire et al. [7] improved their approach to allow for two-phase flow at both pore and continuous scales. The effects of gravity and capillarity in the porous medium are described and numerically implemented in detail in [5]. Also, the test cases and tutorials could be found as an open-source solver (hybridPorousInterFoam) in OpenFOAM, which is used in this present research work.

Test cases and tutorials are provided as an open source decompiler

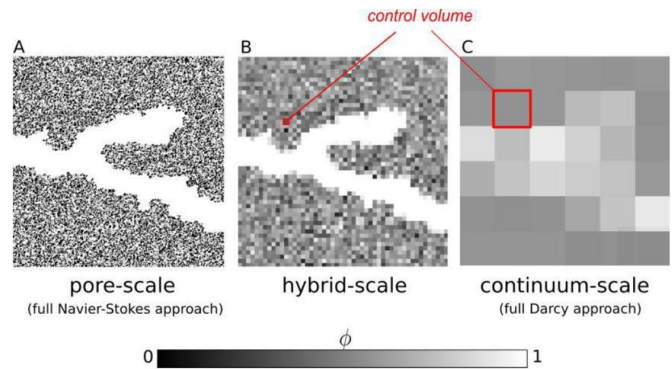


Fig. 1 Graphic representation of a complex porous medium with pore sizes depending on the resolution scale: (a) full pore scale (Navier-Stokes), (b) hybrid scale, and (c) continuous full scale (Darcy) [5].

The main reason to develop this study is to evaluate different fluid properties to understand the flow behavior in complex geometries. For this reason, it is necessary to validate the application of the solver that we could use for the study. The final application of this study is oriented to simulate the injection of water with low salinity concentration, as part of fluid properties in complex porous systems, based in real geometry obtained of micro-CT images of sandstone cores, and determinate the oil recovery factor due to this displacement mechanics.

The paper is divided into five sections, including introduction, the mathematical discretization model, the numerical approach, analysis of the results and discussion about it, and finally the conclusions and recommendations of the investigation.

II. MATHEMATICAL MODEL

In this section is developed the main equations governing multiphase flow at the pore scale. Their components of porous

Digital Object Identifier (DOI):

<http://dx.doi.org/10.18687/LACCEI2022.1.1.369>

ISBN: 978-628-95207-0-5 ISSN: 2414-6390

medium include the solid surface and fluid which include gas-liquid system or liquid-liquid system. The hybridPorousInterFoam is valid for both systems. Is necessary to say that in both systems of is the wetting phase and the other is the non-wetting phase.

The mass conservation in each phase is:

$$\nabla \cdot v_i = 0, \quad (1)$$

where v_i is the velocity of phase i (liquid or gas). Mass conservation at the fluid-fluid interface yields

$$\rho_l(v_l - w) \cdot n_{lg} = \rho_g(v_g - w) \cdot n_{lg} \text{ at } A_{ij}, \quad (2)$$

where ρ_i is phase i density, w is the interface velocity, and finally n_{ij} is fluid-fluid interface normal vector, for wetting to the non-wetting phase. In the fluid-fluid interface, in the absence of phase change the velocities are the same: $v_l = v_g = w$.

Momentum conservation in each fluid is:

$$0 = -\nabla p_i + \rho_i g + \nabla \cdot S_i \quad \text{in } V_i, i = l, g, \quad (3)$$

where g is the gravity vector, $S_i = \mu_i(\nabla v_i + \nabla v_i^T)$ is the viscous stress tensor, and p_i and μ_i are the pressure and viscosity of phase i , respectively. In (3), using the Stokes equation the momentum equation is simulated, also is neglected the inertia force. The Stokes equation is used for its simplicity in the derivation of the micro-continuum momentum equation.

Then, the momentum conservation at the fluid-fluid interface is defined as:

$$[p_l I - S_l] \cdot n_{ln} = [p_g I - S_g] \cdot n_{ln} + \sigma k n_{ln} \quad \text{at } A_{ln}, \quad (4)$$

here I is the unity tensor, σ is the fluid-fluid interfacial tension, and $k = \nabla \cdot n_{lg}$ is the interface curvature. The algebraic discretization of the partial differential equations describing the conservation laws, Eqs. (1) and (3), are performed by integrating over each discrete volume V . This procedure is carried out using the volume averaging operator.

$$\bar{B}_i = \frac{1}{V} \int_V B_i dV. \quad (5)$$

The porosity field ϕ is defined as $(V_l + V_g)/V$, i.e., the volume occupied by both fluids divided by the control volume V , such that:

$$\phi = \begin{cases} 1, & \text{in solid-free regions,} \\ (0; 1), & \text{in porous regions.} \end{cases} \quad (6)$$

The saturation field α_i is defined as $V_i/(V_l + V_g)$, i.e., the volume of liquid divided by the volume occupied by both fluids within the control volume, such that

$$\alpha_i = \begin{cases} 0, & \text{in regions saturated with gas,} \\ (0; 1), & \text{in unsaturated regions,} \\ 1, & \text{in regions saturated with liquid.} \end{cases} \quad (7)$$

The two-phase microcontinuum approach (Darcy-Brinkman) is based in variables with single-field, for example a single fluid velocity and pressure fields, that are identified throughout the network, regardless of the nature of the phases occupying the cells. The pressure (\bar{p}) and velocity (\bar{v}) are defined as weighted sums of:

$$\bar{p} = \alpha_l \bar{p}_l^l + \alpha_g \bar{p}_g^g, \text{ and} \quad (8)$$

$$\bar{v} = \phi [\alpha_l \bar{v}_l^l + \alpha_g \bar{v}_g^g], \quad (9)$$

The sum of the filtration (Darcy) velocities in each phase $\bar{V} = \bar{v}_l + \bar{v}_g$.

The governing equations solving for \bar{p} and \bar{v} are obtained using a strategy in two steps. The first step consist in the volume averaging operator, equation (1), is applied to the continuity equations in (3), and to the momentum equations, equations (3). This results in two differential equations that solve for α_i, \bar{v}_i^i , and \bar{p}_i^i ($i = l, g$). The second step consist in obtain the governing equations of the single field variables, the pairs of averaged phase equations must be added. The explanation in detailed is made in [5], [8]. In biphasic flow, the discontinuity in porosity leads to a change in the shape of the surface tension force. Horgue et al. [6] solves this discontinuity by assuming that the fluid-fluid interface of a droplet on a porous region forms a contact angle θ with the solid surface (see Fig. 2). The contact angle depends on several properties, such as interfacial forces, surface roughness, and the presence of thin precursor films. For this study, the contact angle is within the orientation of the liquid interface relative to the solid surface [5], [8].

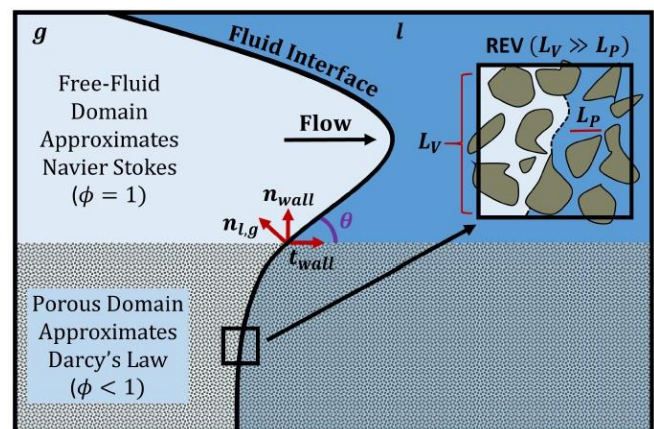


Fig. 2 Conceptual Representation of the multiphase DB micro-continuum approach. θ represents the contact angle and a Representative Elementary Volume (REV) [5].

The relative velocity follows the relation:

$$F_c = \begin{cases} C_e \max(|\bar{p}|) \frac{\bar{v}_{ei}}{\bar{v}_g}, & \text{in clear fluid regions} \\ \phi^{-1} \left[-\left(\frac{M_l}{\alpha_l} - \frac{M_g}{\alpha_g}\right) \bar{v}_p + \left(\frac{\rho_l M_l}{\alpha_l} - \frac{\rho_g M_g}{\alpha_g}\right) g + \left(\frac{M_l \alpha_g}{\alpha_l} + \frac{M_g \alpha_l}{\alpha_g}\right) \bar{v}_{pc} - \left(\frac{M_l}{\alpha_l} - \frac{M_g}{\alpha_g}\right) p_c \bar{v}_{\alpha_l} \right], & \text{in porous regions} \end{cases} \quad (10)$$

The single-field relative permeability is given by:

$$F_c = \begin{cases} 0, & \text{in solid - free regions} \\ k_0^{-1} \left(\frac{k_{r,l}}{\mu_l} + \frac{k_{r,g}}{\mu_g} \right)^{-1}, & \text{in porous regions} \end{cases} \quad (11)$$

The body force F_c describes the capillary forces within a computational cell using:

$$F_c = \begin{cases} -\phi^{-1} \sigma \nabla \cdot (\hat{n}_{lg}) \nabla \alpha_l, & \text{in solid - free regions,} \\ \left[M^{-1} (M_l \alpha_g - M_g \alpha_l) \left(\frac{\partial p_c}{\partial S} - p_c \right) \right] \nabla \alpha_l, & \text{in porous regions} \end{cases} \quad (12)$$

where the modified normal at the fluid-fluid interface is:

$$F_c = \begin{cases} -\frac{\nabla \alpha_l}{|\nabla \alpha_l|}, & \text{in solid - free regions,} \\ \cos \theta n_{\text{wall}} + \sin \theta t_{\text{wall}}, & \text{at the interface between solid - free and porous regions.} \end{cases} \quad (13)$$

Finally, the single-field fluid density is expressed as:

$$\rho = \begin{cases} \rho_l \alpha_l + \rho_g \alpha_g, & \text{in solid - free regions,} \\ (\rho_g M_g + \rho_l M_l) M^{-1}, & \text{in porous regions.} \end{cases} \quad (14)$$

Where the relative permeability is k_{ri} , and M_i is the mobility of the fluid and p_c is the capillary pressure.

III. NUMERICAL APPROACH

A. Solver methodology

The solver used in this work is hybridPorousInterFoam which was proposed by Horgue et al. in [5], and is implemented in the open-source CFD platform OpenFOAM. The used solver hybridPorousInterFoam is applicable for modeling multiphase flow at two scales: continuum (Darcy) and pore scale (Navier-Stokes). Fluid-fluid interactions are modeled by a continuous representation of the Darcy Brinkman equation. Also, the solver evaluated use a single conservation of momentum equation. This solver works using partial differential equations with the finite-volume method for two-phase multi-scale micro-continuum in complex porous media. The main useful advantage of the solver is that it solves the coupled equations using sequential approaches, such as velocity-pressure coupling. The hybridPorousInterFoam solver can be downloaded or accessed from <https://github.com/Franjcf>.

B. Mesh

In the first and second case, 2000 cells is modeled in one

dimension. For the study case, is used 1700 by 760 cells (1 292 000 elements).

C. Boundary Conditions

In the first and second case, water is injected into an air-saturated reservoir at a constant flow rate with the following boundary conditions: $v_{\text{water}} = 1 \times 10^{-5} \text{ms}^{-1}$, $\frac{\partial p_{\text{inlet}}}{\partial x} = 0 \text{Pa m}^{-1}$, and $p_{\text{outlet}} = 0 \text{Pa}$. As water flows into the reservoir, it creates a saturation profile characterized by a water impingement at its front, an effective impingement velocity, and a saturation gradient behind the front. For case 3, the boundary conditions are: water injection velocity = $0.1 \frac{\text{m}}{\text{s}}$, $\theta_{\text{oil}} = 45^\circ$ (water wet system), $p_{\text{outlet}} = 0 \text{Pa}$.

D. Geometry

The geometry is evaluated as a parameter, this is a results of micro-CT cores images. In case 1, BuckleyLeverett's semi-analytical solution was analyzed for air and water flow in a horizontal system with one dimension of 4 mm length without capillary effects. For case 2, the same air-saturated system is tested, but this time with the addition of gravity in the same direction as the water injection rate. Under these conditions, gravity becomes the dominant driving force. In case 3, oil drainage in a complex porous network is tested, the geometry is a complex cross-section system with 1.7 by 0.76 mm dimensions, 1700 by 760 cells, $\phi = 0.001$. and $\kappa_0 = 1 \times 10^{-7} \text{m}^2$. Here, the porosity is fixed at one in the space occupied by the fluid and close to zero in the space occupied by the rock as can be seen in Fig. 3.

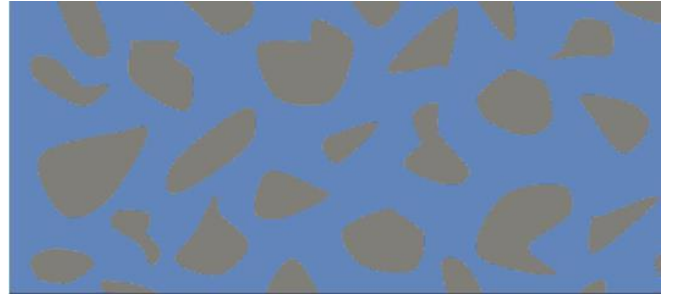


Fig. 3 Graphical representation of oil drainage. The shaded parts represent solid grains, and the blue and red colors represent oil and water, respectively [5].

E. Reynolds Number (Re)

The Reynolds number is a value used to characterize the motion of a fluid and predict the transition from laminar to turbulent flow. It is defined as the ratio of the product of the velocity by the core length divided by the kinematic viscosity of the fluid [9]. Inertial effects are important when there are changes in flow direction and are proportional to that velocity. For Reynolds numbers greater than 1000, it is observed that the friction factor is a constant and no longer depends on it, and the inertial effects will dominate the flow of fluids. For

Reynolds number values between 1 and 1000, it is considered within the transition flow.

IV. RESULTS AND DISCUSSION

In this section, it was verified that the hybridPorousInterFoam solver effectively converges towards its two asymptotic limits, in comparison to the results obtained in [5] and [8]. The properties of the fluids used in this paper were obtained from Horgue et.al [8] and are shown in Table I.

TABLE I
TABLE OF FLUID PROPERTIES [8].

Property	Value	Units
Water Density	1000	Kg m ⁻³
Water Viscosity	1 x 10 ⁻³	Pa s
Air Density	1	Kg m ⁻³
Air Viscosity	1.76 x 10 ⁻⁵	Pa s
Oil Density	800	Kg m ⁻³
Oil Viscosity	0.1	Pa s
Gravity	9.81	m s ⁻²

A. Case 1: Buckley-Leverett semi-analytical solution

In this case, initially, the reservoir is saturated with air, then water is injected at a constant flow rate ($v=1 \times 10^{-5} \text{ ms}^{-2}$). As water invades the reservoir, it creates a saturation profile characterized by the water impact in front of it, an effective impingement velocity, and a saturation gradient behind said front shown in Fig. 4. While water is injected, it generates a small interface, which can be seen as a white line in which the water saturation changes from one to zero as we can see in Fig. 4 (a). In Fig. 4 (b) we can see the interface in line black as a result of the solver validation. This is explained because these two fluids are miscible. Fluid-fluid interface increases depending on the type of fluid, for example, when oil is displaced by water, is possible to observe micro emulsions. In this case, the effect of gravity is not considered, and this assumption implies that the water saturation is 100%.

B. Case 2: Oil drainage in a complex pore network

Although the evaluated system derives from the previous case, on a small scale the complexity lies in the initialization of the heterogeneous porosity field, this as a representation of the cross-section assuming that it is an oil-wet rock. It settles to a value of one of the cells occupied by the liquid and close to zero in the cells occupied by the rock. This condition allows the simulation of solid grains acting as impermeable surfaces [6]. To verify the accuracy of the solver used, the tutorial was initially run and compared with the results obtained by the author under the same simulation conditions. Fig. 5 shows the results obtained in [5], and the results of the validation process in this study, these two results are very identical, due to the same fluid paths and the same droplet detachment at

simulation time step 5 ms. However, there are slight differences in the graphical results, with some interfaces scrolling at slightly different speeds than their counterparts (see top right corner at simulation time 10 ms) [10].

C. Case Study: Change in Reynolds Number for complex porous medium

It is usual to compare dimensionless numbers such as a Reynolds Number, for a better understanding of the fluid flow behavior in a complex porous medium as is shown in Fig. 6 when time is 0.0065 s (this time refers to computational times, because the number of 292 000 elements). For the case in which the Reynolds number is 0.1 times the initial case (b), the results indicate that displacement of the oil by water is less effective due to the increase of viscous forces. According to the Darcy equations, if the viscosity number tends to be zero in light oil, in contrast, if the viscosity number increases the velocity of flux reduces as is shown in (a). On the other hand, when the Reynolds number is ten times higher than the initial case, the fluid saturation has the same behavior that in the base case (b), but with the difference that advances and saturated more pore through., as we can see in Fig. 6 (c). In conclusion, the fluid properties influenced the fluid flow in a complex porous medium.

V. CONCLUSIONS

The hybridPorousInterFoam solver enables multiphase flow modeling in complex porous media with high accuracy, mainly because it incorporates micro- to macro-scale scaling including the effects of porous media surface heterogeneity and different interaction forces across the field. of pressures and velocities in each cell of the case study.

The fluid properties influenced the fluid flow in a complex porous medium, it is observed when the Reynold number was changed, and this behavior is in concordance of fluid flow at the microscale (pore-scale). For low Reynolds numbers, the Darcy regime is observed, as the Reynolds number increases, the inertial effects become more important. It is important, to continue investigating other properties to understand the oil recovery using hybridPorusInterFoam.

The present work allowed us to validate the use and the potentiality of the solver hybridPorousInterFoam. It is necessary to investigate the stability of the fluid flow and this should be independent of the mesh, that is, to reach the same state of convergence before continuing with the simulations. Likewise, it is necessary to include qualitative analyzes for better comparisons, using dimensionless numbers, such as the Darcy number and the Capillary number adding to the Reynolds number.

ACKNOWLEDGMENT

The authors thanks to Fondo Nacional de Desarrollo Científico, Tecnológico y de Innovación Tecnológica (FONDECYT) (Perú) for the financial support provided during the development of this work. Likewise, to the Research Institute of the Faculty of Petroleum, Natural Gas and Petrochemical Engineering, of the Universidad Nacional de Ingeniería.

REFERENCES

- [1] B. P. Scandella, k. Delwiche, H. F. Hemond and R. Juanes, "Persistence of bubble outlets in soft, methane-generating sediments.," *Journal of Geophysical Research: Biogeosciences*, pp. 122, 1298-1320., 2017.
- [2] A. Q. Raeini, B. Bijeljic and M. J. Blunt, "Numerical modelling of sub-pore scale events in two-phase flow through porous media.," *Transport in porous media*, pp. 101(2), 191-213., 2014.
- [3] R. Aziz, V. Joekar-Niasar, P. J. Martínez-Ferrer, O. E. Godínez-Brisuela, C. Theodoropoulos and H. Mahani, "Novel insights into pore-scale dynamics of wettability alteration during low salinity waterflooding.," *Scientific reports*, pp. 9(1), 1-13., 2019.
- [4] Z. Alhashmi, M. J. Blunt and B. Bijeljic, "The impact of pore structure heterogeneity, transport, and reaction conditions on fluid-fluid reaction rate studied on images of pore space.," *Transport in Porous Media*, pp. 115(2), 215-237., 2016.
- [5] F. J. Carrillo, I. C. Bourg and C. Soulaine, "Multiphase Flow Modelling in Multiscale Porous Media: An Open-Sourced Micro-Continuum Approach.," *arXiv preprint arXiv:2003.08374*, 2020.
- [6] P. Horgue, M. Prat and M. Quintard, "A penalization technique applied to the "Volume-Of-Fluid" method: Wettability condition on immersed boundaries.," *Computers & Fluids*, pp. 100, 255-266., 2014.
- [7] C. Soulaine, P. Creux and H. A. Tchepi, "Micro-continuum framework for pore-scale multiphase fluid transport in shale formations.," *Transport in Porous Media*, pp. 127(1), 85-112., 2019.
- [8] P. Horgue, C. Soulaine, J. Franc, R. Guibert and G. Debenest, "An open-source toolbox for multiphase flow in porous media.," *Computer Physics Communications*, pp. 187, 217-226., 2015.
- [9] B. L. White y H. M. Nepf, «Shear instability and coherent structures in shallow flow adjacent to a porous layer.» *Journal of Fluid Mechanics*, vol. 593, pp. 1-32, 2007.
- [10] K. Singh, "How Hydraulic Properties of Organic Matter Control Effective Liquid Permeability of Mudrocks.," *Transport in Porous Media*, pp. 129(3), 761-777., 2019.

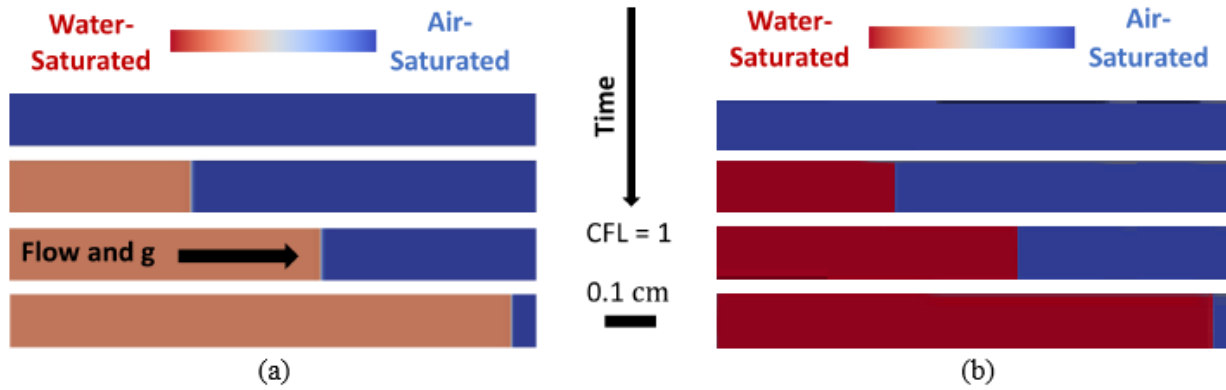


Fig. 4 Water saturation in the reservoir over time, (a) show the results obtained in [5], and in (b) show the results obtained in this investigation

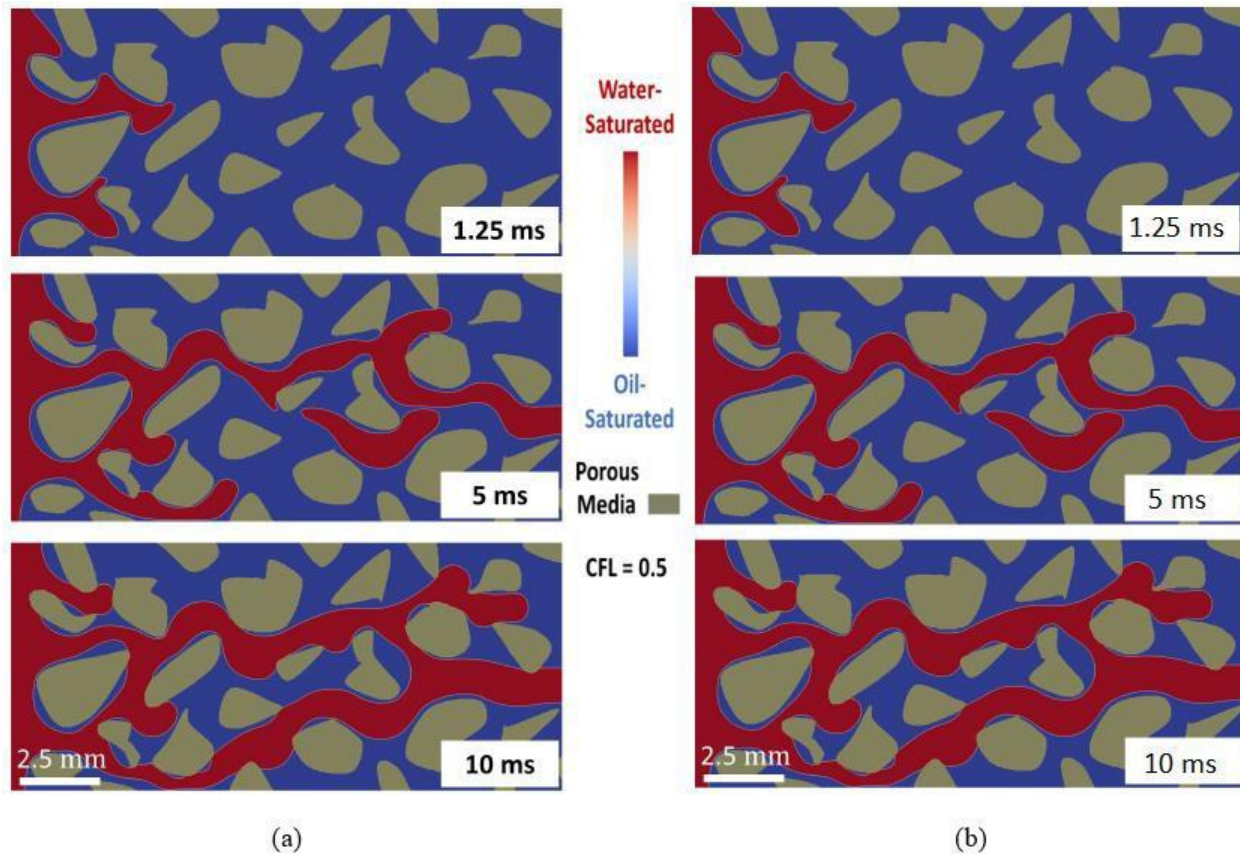


Fig. 5 Oil drainage in a complex porous medium solved at the pore scale using hybridPorousInterFoam. The shaded sections represent solid grains, and the blue and red colors represent oil and water, respectively.

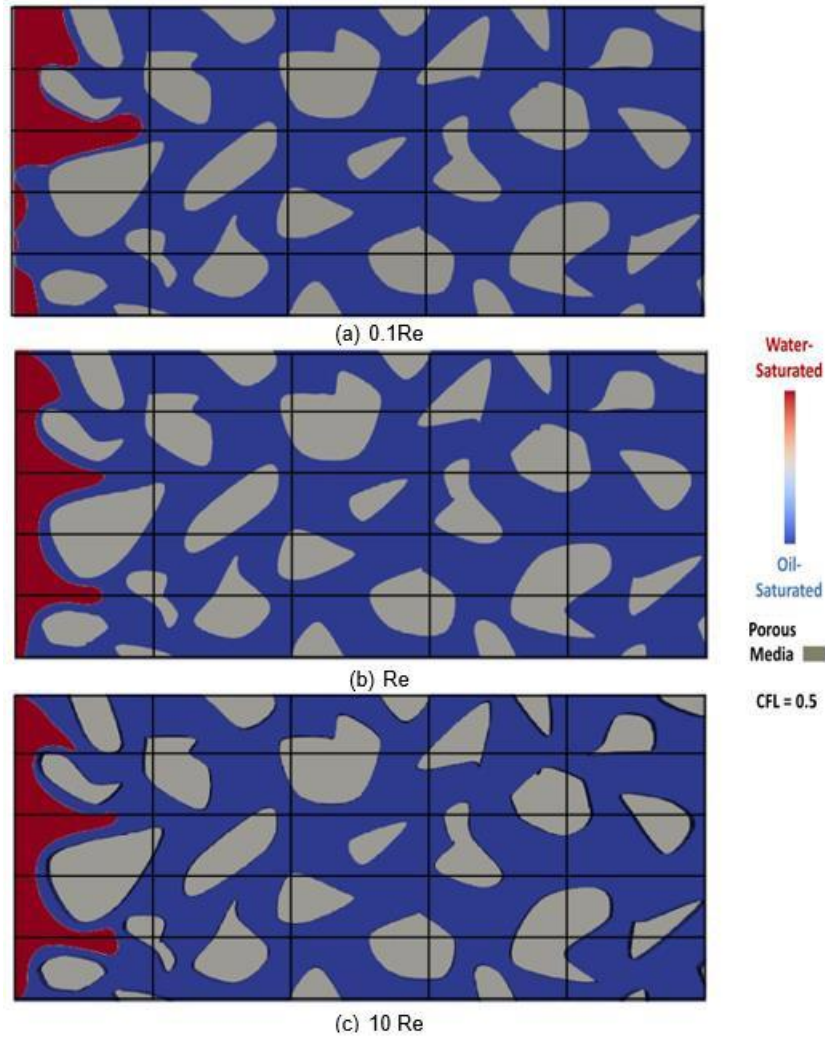


Fig. 6 Change in Reynolds Number for complex porous medium: (a) 0.1Re, (b) Re and (c) 10 Re